European Journal of Heart Failure (2016)
doi:10.1002/ejhf.463

A specifically designed nanoconstruct associates, internalizes, traffics in cardiovascular cells, and accumulates in failing myocardium: a new strategy for heart failure diagnostics and therapeutics

Guillermo U. Ruiz-Esparza[1,2,3], Victor Segura-Ibarra[1,2], Andrea M. Cordero-Reyes[4], Keith A. Youker[4], Rita E. Serda[5], Ana S. Cruz-Solbes[4], Javier Amione-Guerra[4], Kenji Yokoi[1], Dickson K. Kirui[1], Francisca E. Cara[1], Jesus Paez-Mayorga[3], Jose H. Flores-Arredondo[5], Carlos E. Guerrero-Beltrán[3], Gerardo Garcia-Rivas[3], Mauro Ferrari[1,6], Elvin Blanco[1†*], and Guillermo Torre-Amione[3,4†*]

[1]Department of Nanomedicine, Houston Methodist Research Institute, 6670 Bertner Street, MS R7-360.5, Houston, TX 77030, USA; [2]Escuela de Ingeniería y Ciencias, Tecnológico de Monterrey, Monterrey N.L., México 64849; [3]Catedra de Cardiología y Medicina Vascular, Escuela Nacional de Medicina, Tecnológico de Monterrey, Monterrey N.L., México 64710; [4]DeBakey Heart and Vascular Center, Houston Methodist Hospital, 6565 Fannin Street, Suite 1901, Houston, TX 77030, USA; [5]Michael E. DeBakey Department of Surgery, Baylor College of Medicine, Houston, TX 77030, USA; and [6]Department of Medicine, Weill Cornell Medical College New York, NY, 10021, USA

Received 5 May 2015; revised 24 September 2015; accepted 12 November 2015

Aims Ongoing inflammation and endothelial dysfunction occurs within the local microenvironment of heart failure, creating an appropriate scenario for successful use and delivery of nanovectors. This study sought to investigate whether cardiovascular cells associate, internalize, and traffic a nanoplatform called mesoporous silicon vector (MSV), and determine its intravenous accumulation in cardiac tissue in a murine model of heart failure.

Methods and results *In vitro* cellular uptake and intracellular trafficking of MSVs was examined by scanning electron microscopy, confocal microscopy, time-lapse microscopy, and flow cytometry in cardiac myocytes, fibroblasts, smooth muscle cells, and endothelial cells. The MSVs were internalized within the first hours, and trafficked to perinuclear regions in all the cell lines. Cytotoxicity was investigated by annexin V and cell cycle assays. No significant evidence of toxicity was found. *In vivo* intravenous cardiac accumulation of MSVs was examined by high content fluorescence and confocal microscopy, with results showing increased accumulation of particles in failing hearts compared with normal hearts. Similar to observations *in vitro*, MSVs were able to associate, internalize, and traffic to the perinuclear region of cardiomyocytes *in vivo*.

Conclusions Results show that MSVs associate, internalize, and traffic in cardiovascular cells without any significant toxicity. Furthermore, MSVs accumulate in failing myocardium after intravenous administration, reaching intracellular regions of the cardiomyocytes. These findings represent a novel avenue to develop nanotechnology-based therapeutics and diagnostics in heart failure.

Keywords Heart failure • Cardiomyopathy • Nanotechnology • Nanomedicine • Nanoconstructs • Nanoparticles

*Corresponding author: Tel: +1 713 441 2762; Fax: +1 713 790 2643; Email: gtorre@tecsalud.mx/ Tel: +1 713 441 7437; Fax: +1 713 441 7438; Email: eblanco@HoustonMethodist.org
†These authors share senior authorship.

Introduction

Despite the fact that conventional therapeutics such as angiotensin-converting enzyme (ACE) inhibitors, angiotensin receptor antagonists (ARBs), and diuretics are able to reach the site of action and expand the lifespan of a patient with chronic heart failure, treatment with other kinds of small molecules and/or genetic material remains a challenge. Clinical use of the latter agents remains limited, hindered by the inability to achieve high drug concentrations within the myocardium because of systemic side-effects or by the lack of efficient non-invasive methods for gene delivery.[1,2] Novel delivery strategies into failing myocardium may improve current diagnostic and therapeutic potential.

The rise of nanotechnology has led to the creation of platforms that are capable of passively and actively increasing local drug concentration and has even made possible the delivery of genetic material (siRNA, pDNA, mRNA, etc.) as therapeutic agents. Although these discoveries have been mostly applied in the cancer therapy, research suggests that the same conditions that are present in the tumour microenvironment, such as disrupted endothelium and hyperpermeability, may also be present in other pathologies, one of them being chronic heart failure. Following intravenous administration of nanoparticles in tumour-bearing animals, there is an increase in accumulation of those particles within the tumour compared to healthy and non-fenestrated tissues. This phenomenon occurs as a direct result of an increase in tumour vascular permeability not seen in other tissues, for example the normal heart.[3] In cardiovascular applications, a published report in an experimental model of myocardial infarction demonstrates increase in nanoparticle accumulation in the peri-infarct zone, as a result of changes in vascular permeability.[4,5]

The heart failure milieu is characterized by local inflammation, hypoxia, oxidative stress, impaired lymphatic drainage, and impaired recovery of cardiac contractibility—conditions similar to those observed in the tumour micro-environment and in the peri-infarct zone of myocardial infarction.[3,6–9] If indeed those conditions result in changes in vascular permeability, it is likely that following intravenous administration of nanoparticles in heart failure, they may extravasate from blood vessels and reach the failing myocardium. Accordingly, we aimed to determine whether a nanoconstruct administered intravenously would accumulate and be retained in failing myocardium.

To test this hypothesis a nanostructured discoidal mesoporous silicon vector (MSV) with dimensions of 1000×400 nm loaded with ~10 nm polymeric nanoparticles was used to first determine the kinetics of MSV association and attachment to the cellular membrane, internalization to the cytoplasm, and intracellular trafficking in primary cardiovascular cell lines, and second to determine whether MSVs accumulated in failing myocardium following *in vivo* intravenous administration.

Methods

Mesoporous silicon vector fabrication and assembly of fluorescent nanoparticles

The MSVs were fabricated using photolithography and electrochemical etching.[10] Slightly negatively charged ~10 nm polymeric nanoparticles loaded with a fluorescent dye (excitation 630 nm, emission 650 nm) were fabricated as described previously.[11] The fluorescent nanoparticles were then loaded into positively charged pores of MSVs by mixing followed by sonication. Details provided in the Supplementary material online, *Methods S1*.

Cardiovascular cell lines

Human primary cell lines, cardiomyocytes (HCM), cardiac fibroblasts (HCF), coronary artery smooth muscle cells (HCASMC), and cardiac microvascular endothelial cells (HCMEC) were purchased from PROMOCELL (Manassas, VA, USA). Primary rat cardiomyocytes (RCM) were isolated and maintained according to a previously established protocol.[12] Media was purchased from PROMOCEL. All human cell lines were used within the first 10 passages of culture and maintained at 37°C in a humidified atmosphere containing 5% CO_2.

Scanning electron microscopy examination of mesoporous silicon vector–cell membrane interaction

Extracellular interaction between cells and MSVs, such as particle–membrane association, actin filament rearrangement, and membrane engulfment of particles, was examined by a Nova NanoSEM 230 system (FEI, Hillsboro, OR, USA). After the cell incubation period, MSVs were administered in a ratio of 25 particles per cell (3.8 μg/mL). Details are provided in the Supplementary material online, *Methods S1*.

Examination of cellular uptake and subcellular localization of mesoporous silicon vectors by confocal microscopy

To determine cellular uptake and subcellular localization of MSVs, cardiovascular cell lines were seeded into eight-well chamber culture slides (BD Biosciences, Franklin Lakes, NJ, USA) and incubated with a ratio of 25 MSVs per cell (3.8 μg/mL). Cells were collected at predetermined time-points, fixed, and stained. Images were obtained using a Nikon A1 confocal microscopy system (Nikon Instruments, Melville, NY, USA). Details provided in the Supplementary material online, *Methods S1*.

Flow cytometry analysis of cellular uptake kinetics of mesoporous silicon vectors

To determine MSV uptake kinetics, HCM, HCF, HCASMC, HCMEC, and RCM were seeded in six-well plates (BD Biosciences, San Jose, California, USA) and incubated with the fluorescently loaded MSVs. At predetermined time-points, 1.0×10^7 cells were collected, and evaluated by flow cytometry, acquiring 10 000 events per time-point. Side scatter measurements were performed using a LSRFortessa Flow Cytometer (BD Biosciences, San Jose, California, USA), equipped with a 630 nm laser. Details are provided in the Supplementary material online, *Methods S1*.

In vitro toxicity of mesoporous silicon vectors

Apoptosis and necrosis caused by MSVs were evaluated in human cell lines. Cells were seeded in six-well plates and incubated for 24 h

with the following MSV concentrations (cell to particle ratio): 1:1 (0.2 μg/mL), 1:25 (5 μg/mL), 1:150 (30 μg/mL), and 1:250 (50 μg/mL). Cells were labelled using the Annexin V Apoptosis Detection kit FITC (eBioscience, San Diego, CA, USA), and flow cytometry was performed. Details provided in the Supplementary material online, *Methods S1*.

Determination of cell cycle progression after administration of mesoporous silicon vectors

To determine if MSVs caused cell cycle alterations, cell lines were plated into six-well plates at 70% density and incubated for 24 h with the same dose ranges as the cytotoxicity assay. Cells were collected and stained with a solution of propidium iodide (5 μg/mL), further analysis using flow cytometry was performed as described previously, acquiring 20 000 events per well. Details provided in the Supplementary material online, *Methods S1*.

In vivo study design

All animal experiments were reviewed and approved by the Institutional Animal Care and Use Committee of the Houston Methodist Research Institute. All experiments were performed in male C57BL/6 purchased from Harlan Laboratories (Indianapolis, IN, USA). To examine the *in vivo* accumulation dynamics of MSVs, a murine model of heart failure was used, the animal model consisted of 1 week *ad libitum* administration of water containing 1% NaCl and 0.01% of *N*-nitro L-arginine methyl ester (l-NAME), then a micro-osmotic pump was surgically implanted in the subdermal dorsal area, diffusing angiotensin II at a rate of 0.7 mg/kg.day over a course of 14 days.[13] At the fifth week heart failure was induced and all *in vivo* experiments were performed. This model demonstrates parameters of cardiac dysfunction, such as the increase of hormones associated with heart failure (elevation of BNP), changes in inflammatory markers, adverse remodelling, depression in ejection fraction and cardiomyopathy, characteristic of heart failure.[14] For the purpose of this study two sets of animals were used: (i) mice with normal hearts ($n = 15$); and (ii) mice with induced heart failure ($n = 15$). Each set was divided into two experimental groups: non-treated mice ($n = 5$) and MSV-treated mice ($n = 10$). Treated groups received 1×10^9 MSVs (0.2 mg) administered intravenously. Non-treated groups received phosphate-buffered saline (PBS). After 24 h, mice were sacrificed and heart tissues extracted, frozen, and sectioned into 7 μm sagittal and transversal slices using a HM550 Cryostat system (Thermo Fischer Scientific, Waltham, MA, USA).

Wide-field imaging of heart tissues

To determine accumulation and homogeneity of MSVs in different cardiac regions, complete sagittal and transverse frozen sections of normal and failing hearts were captured using an ImageXpress Micro XLS wide-field high-content fluorescence imaging system (Molecular Devices, Sunnyvale, CA, USA). Details are provided in the Supplementary material online, *Methods S1*.

Confocal examination and quantification of mesoporous silicon vectors in heart tissues

To determine cellular and subcellular localization of MSVs, staining of endothelial cells and cardiomyocytes present in transverse and sagittal heart tissue sections was performed. Images from 10 normal and 10 failing hearts were captured, in which four regions of each heart were imaged and analysed using z-stacking and tridimensional rendering through NIS Elements v4.1 software (Nikon Instruments, Melville, NY, USA). Area fraction was determined by the fluorescence emitted on the 403, 488, and 561 nm channels. The MSVs (630 nm), were individually quantified by using the automatic counting tool from the NIS-Elements software. To calculate the amount of particles present per square inch, the quantified number of MSVs was normalized by surface area of the tissue in each image. Details are provided in the Supplementary material online, *Methods S1*.

Organ biodistribution

To determine accumulation in organs, three animals undergoing heart failure were injected with 1×10^9 MSVs loaded with fluorescent polymeric nanoparticles (Bodipy: excitation 630 nm, emission 650 nm). The animals were then sacrificed at the 24 h time-point and organs harvested to be analysed by measuring epifluorescence using an *in vivo* imaging system IVIS Caliper-200 (PerkinElmer, Akron, OH, USA).

In vivo cardiotoxicity of mesoporous silicon vectors

To assess *in vivo* cardiotoxicity of MSVs, animals with induced heart failure were administered 1×10^9 MSVs and echocardiograms were performed 24 h after injections using a Vevo 770 High-Resolution *In Vivo* Micro-Imaging System (Toronto, ON, Canada).

Statistical analysis

Results are expressed as mean ± SE. Differences between two groups were analysed using an unpaired *t*-test, assuming unequal variants. A value of $P < 0.001$ was considered significant. Statistics were calculated using GraphPad Prism software (La Jolla, CA, USA).

Results

Cellular association and internalization of mesoporous silicon vectors by cardiovascular cells

Figure 1 shows association and internalization of MSVs over time in HCM, HCF, CASMC, HCMEC, and RCM. Cell membrane association of MSVs was observed after 15 min of administration in all cell types (*Figure 1A*). After the second hour of incubation, pseudopodia and membrane extroflessions formed, resulting in MSV engulfment (*Figure 1B*). Internalization of the MSVs by all cardiovascular cell lines was further supported by confocal z-stack acquisition at 24 h, confirming the presence of particles beneath the cellular membrane (*Figure 1C*). The Supplementary material online, *Figure S1*, contains tridimensional reconstructions of human cell types.

Figure 2 shows particle uptake kinetics in HCM, HCF, CASMC, HCMEC, and RCM. *Figure 2A,B* shows confocal micrographs captured at 1 h and 120 h, respectively. A progressive accumulation of MSVs within the cardiovascular cells was observed. *Figure 2C* shows cellular uptake dynamics of MSVs by flow cytometry in each cell line

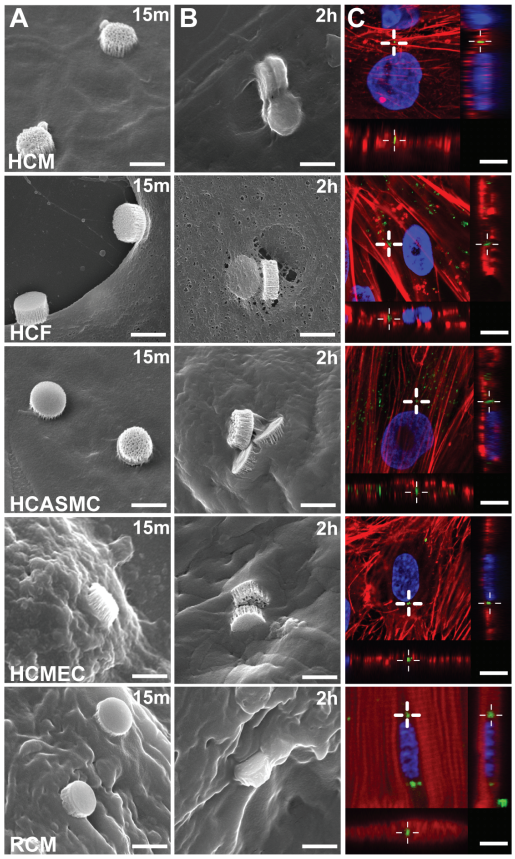

Figure 1 Cellular association and internalization of MSVs. *(A)* Scanning electron micrographs of cardiovascular cells incubated with mesoporous silicon vectors (MSVs) (1:25, Cell:MSV ratio) demonstrating particle adhesion to the cellular membrane after 15 min of administration; bars, 1 µm. *(B)* Extensive cellular membrane rearrangement and engulfment of MSVs following 2 h of incubation; bars, 1 µm. *(C)* Z-stack analysis at 24 h via confocal microscopy demonstrating internalization and co-localization of MSVs beneath the cellular membrane. Actin cytoskeleton was labelled red, nuclear structures blue, and particles are visualized in green; bars, 10 µm.

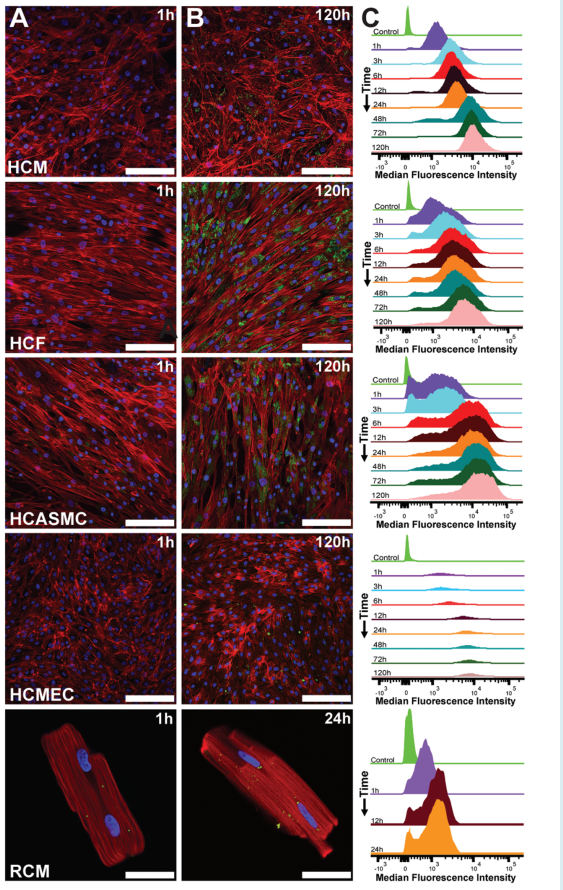

Figure 2 Mesoporous silicon vector (MSV) uptake dynamics. *(A)* Confocal micrographs showing scarce association of MSVs after 1 h of incubation; bars, 100 µm. *(B)* After 120 h in human cardiovascular cell lines and 24 h in rat cardiomyocytes, a gradual increase of nanoconstructs accumulation was observed; bars, 100 µm. Actin cytoskeleton was labelled red, nuclear structures blue, and particles are visualized in green. *(C)* MSV uptake dynamics of cardiovascular cells were measured by flow cytometry at predetermined time-points for human cell types (1, 3, 6, 12, 24, 48, 72, and 120 h) and rat adult cardiomyocytes (1, 12, and 24 h). Results shown are the mean of three independent experiments.

over time. After 1 h, median fluorescence intensity demonstrated that most MSVs were still outside cells. An increase in median fluorescence intensity was observed during the first 48 h in HCM before reaching a plateau. Cardiac fibroblasts presented a less gradual increase of fluorescence, before reaching a saturation point at 72 h. Saturation of uptake occurred earlier in HCASMC, reaching a plateau after 6 h. A similar saturation phenomenon was observed in HCMEC after 12 h of incubation with MSVs. Rat cardiomyocytes showed a plateau in uptake dynamics after 12 h.

Intracellular trafficking and localization of mesoporous silicon vectors

High-magnification confocal micrographs show intracellular trafficking of MSVs in each cell type (*Figure 3*). Within the first hour, MSVs associated with the cellular membrane and underwent internalization in all cardiovascular cells (*Figure 3A*). *Figure 3B* shows that MSVs trafficked to the perinuclear region of the five cell lines. During the first 24 h, HCASMC and HCF accumulated and retained MSVs within the perinuclear region. Perinuclear accumulation was accompanied with a more homogeneous distribution of MSVs in HCM and HCMEC. In RCM after 2 h, MSVs internalized and trafficked to the perinuclear region, as observed in the human cells. In order to confirm this phenomenon, time-lapse microscopy was performed in the four human cardiac cell lines. Images were taken every 20 min for 12 h and videos were compiled. Results confirmed intracellular transport to the perinuclear region of the cells, as well as transport of MSVs between adjacent cells in some cell types (see the Supplementary material online, *Videos S1–S4*).

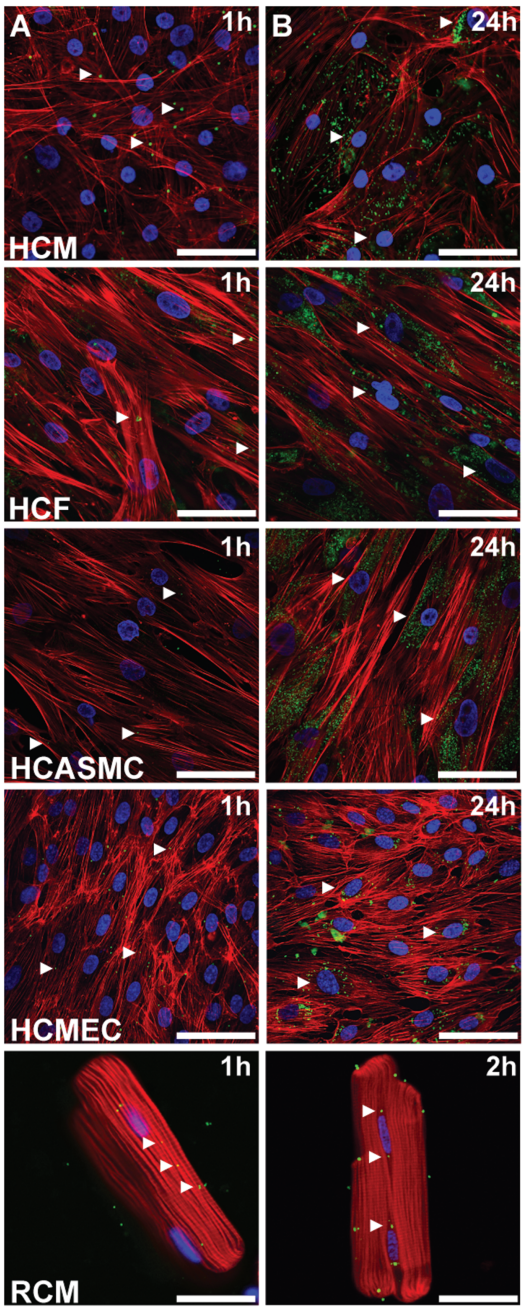

Figure 3 Mesoporous silicon vector (MSV) intracellular trafficking. High-magnification confocal micrographs of cardiovascular cells were obtained and *(A)* at the first hour MSVs were randomly distributed through the cellular membrane and underwent phagocytosis; bars, 40 μm. *(B)* Over time, MSVs trafficked to the perinuclear region of the cells through the microtubules; bars, 40 μm. Actin cytoskeleton was labelled red, nuclear structures blue, and particles are visualized in green.

In summary, HCM showed MSV cellular trafficking to adjacent cells and particle sequestration within perinuclear regions. Human cardiac fibroblasts showed the highest retention and sequestration of MSVs in perinuclear regions compared with other cells. No cellular trafficking of MSVs to adjacent cells was detected in HCF. The HCASMC showed limited MSV trafficking between adjacent cells, with further sequestration of MSVs in its perinuclear region. The HCMEC uptake kinetics were accompanied by MSV trafficking between adjacent cells and limited perinuclear sequestration. The RCM showed MSV internalization and sequestration within its perinuclear region.

In vitro and *in vivo* toxicity of mesoporous silicon vectors

The Supplementary material online, *Figures S2*, *S3* and *S4* show the cytotoxic response of human cardiovascular cells exposed for 24 h to increasing MSV concentrations (cell:MSV: 1:1–1:250). *Figure S4* shows that percentage of necrotic and apoptotic cells was maintained below 2.5% at all doses after 24 h of incubation, as determined by Annexin V assay. To detect alterations in cell cycle progression of cardiac cells, we administered the same MSV dose ranges as the cytotoxicity assay and compared these with untreated control cell populations. The cell cycle progression of MSV-treated cells was not disrupted at different doses (see the Supplementary material online, *Figure S4*). Echocardiograms performed on mice 24 h after administration of 1×10^9 MSVs did not show any effects on myocardial function compared with failing hearts, with the ejection fraction remaining unaffected; this proved that these nanoconstructs do not elicit effects on contractility (data not shown).

Accumulation of mesoporous silicon vectors in the failing heart and other organs

A murine model of heart failure (see the Supplementary material online, *Figure S5*) was used to examine accumulation dynamics of MSVs after intravenous administration. *Figure 4* shows accumulation of MSVs in control normal hearts and failing hearts 24 h after administration. As shown in *Figure 4A*, control hearts showed slight green fluorescence associated with the MSVs, whereas failing heart sections were highly enriched with fluorescence within different regions (*Figure 4B*), indicating increased accumulation of MSVs. The accumulation detected within failing hearts was homogeneously distributed, indicating similar accumulation dynamics within the walls.

The bottom left insets shown in *Figure 4A,B* show microscopic magnifications of the same sections; the increased fluorescence in the failing heart as a result of heightened MSV accumulation is clear. *Figure 4C* shows quantitative analysis of MSVs in normal and failing hearts, showing an average of 172.78 and 2474.79 MSVs/mm^2, respectively. The Supplementary material online, *Figure S6*, shows the *in vivo* organ biodistribution of the MSVs after 24 h of administration (heart, lungs, liver, kidneys and spleen). Findings demonstrate high accumulation of MSVs in organs that comprise the reticuloendothelial system (RES), results that are in agreement with previously published reports from our laboratory.[15–17]

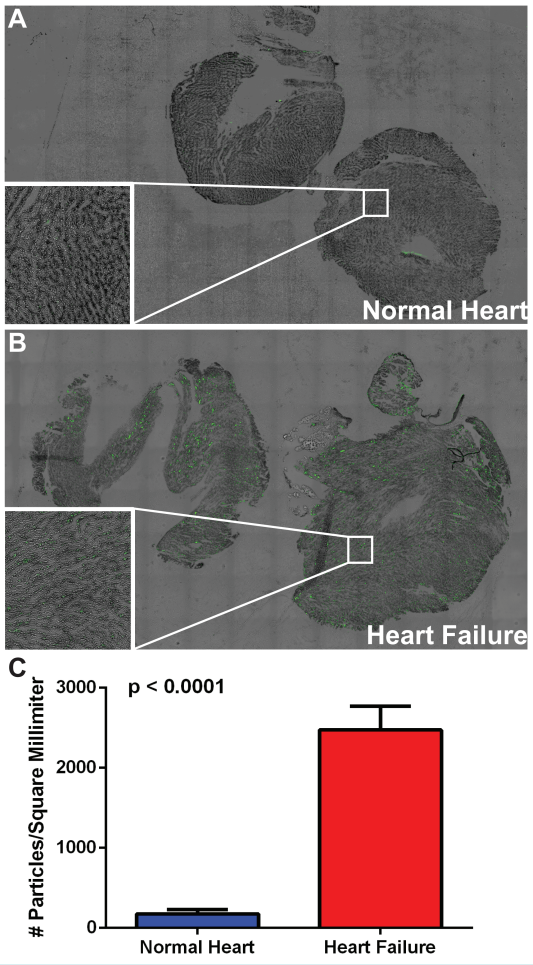

Figure 4 Accumulation of mesoporous silicon vectors (MSVs) in control normal and failing hearts. Twenty-four hours after administration, normal and failing hearts were sectioned in transverse and sagittal planes, and imaged using high-content fluorescent microscopy. *(A)* Control normal cardiac tissue shows slight amount of fluorescence emitted from the MSVs (green). *(B)* In contrast, a significant increase of homogeneously distributed fluorescence associated with the nanoconstructs was detected in the failing heart. Insets show microscopic magnifications of myocardial tissue (nanoconstructs are visualized in green). *(C)* MSVs were quantified by measuring area fraction, surface area in millimetres and automatic particle counting by the microscopy software. A 14-fold increase of MSVs uptake was detected in the failing heart.

Association of mesoporous silicon vectors with cardiomyocytes in failing myocardium

Figure 5 shows cellular localization of MSVs in the failing heart after intravenous administration. As shown in *Figure 5A*, MSVs were able to extravasate through endothelial barriers and reach the failing myocardium with adequate homogenous diffusion. *Figure 5B* shows high magnification fluorescence micrographs demonstrating heightened levels of MSV accumulation in cardiomyocytes. *Figure 5C* shows z-stacking and tridimensional rendering, confirming cellular uptake of MSVs by cardiomyocytes. *Figure 5D* shows that MSVs reached the perinuclear region inside the cardiomyocytes.

Discussion

These findings demonstrate for the first time that nanoconstructs can be taken up by primary cardiac cell lines without toxicity and, furthermore, that they accumulate in higher amounts in the failing myocardium compared to normal heart when intravenously injected. These data provide the necessary first steps to utilizing nanoconstructs for diagnostic or therapeutic purposes in heart failure (*Figure 6*).

Mesoporous silicon vectors were chosen for these studies as they are designed to successfully circumnavigate several biological barriers, enhancing vascular wall margination and cellular uptake.[18] This platform has previously shown enhanced delivery with respect to free nanoparticles because of its protection and controllable sustained release of nanotherapeutics-containing drugs and genetic material within tumours.[11,19]

Mesoporous silicon vectors associate and are internalized by cardiovascular cells

The MSVs associated with, and were internalized in cultured human cell lines, as well as in non-dividing rat cardiomyocytes. Membrane reorganization and formation of pseudopodia with extension of the cellular membrane toward the particles was present in all cell types. Our laboratory has previously examined and thoroughly characterized the internalization mechanism of MSVs in a variety of cell lines (e.g. human umbilical vein endothelial cells), with findings demonstrating that cellular uptake of MSVs occurred via an actin-dependent mechanism involving both phagocytosis and micropinocytosis, which are characterized by reorganization of the actin cytoskeleton, leading to structural changes in the cellular membrane and engulfment of extracellular materials.[20–24] Our observations are consistent with previous studies that documented phagocytosis of other types of material by cardiomyocytes, fibroblasts, smooth muscle cells, and endothelial cells.[25–28]

To further understand uptake kinetics, confocal microscopy and flow cytometry analysis of cardiac cell lines incubated with MSVs, was performed. Confocal micrographs of HCF and HCASMC showed heightened accumulation of MSVs, when compared with HCM and HCMEC. The uptake dynamics of MSVs observed by confocal imaging and flow cytometry demonstrated a time-dependent pattern. Internalization of MSVs increased gradually at early time-points and, as time progressed, a decrease was observed in all cell lines until a plateau was reached. The saturation kinetics resemble adaptive responses of macrophages to their microenvironment wherein an initial response stimulates very efficient phagocytosis and then the initial capacity subsequently diminishes.[29,30]

Subcellular accumulation of MSVs resemble the perinuclear deposition of phagocytic material in cells, a microtubule-mediated system that depends of various motor proteins of the endocytic

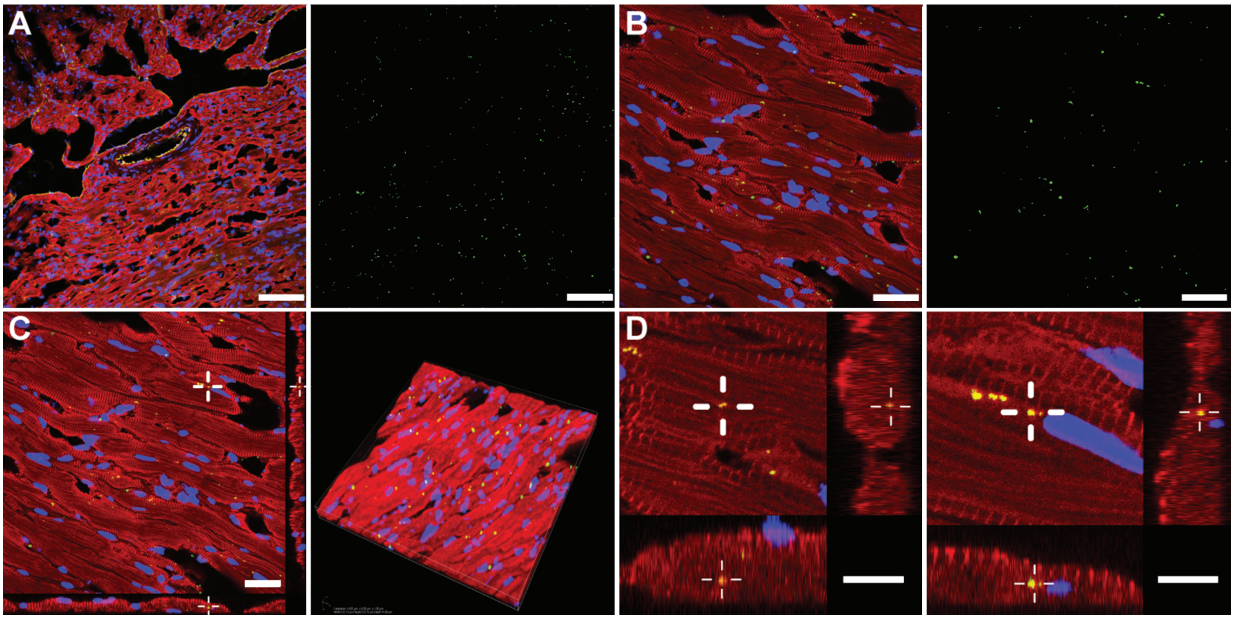

Figure 5 *In vivo* cellular and subcellular localization of mesoporous silicon vectors (MSVs). To evaluate the extravasation of MSVs (green) in the failing heart, sarcomeric actinin of myocardial cells was labelled in red, CD-31-positive vasculature in yellow, and nuclear structures in blue. *(A)* MSVs extravasation across the endothelial barrier was observed and endothelial cells showed minimal accumulation. In contrast, high levels of nanoconstructs were homogeneously co-localized within the cardiomyocytes. Particle fluorescence (green) was extracted from the micrograph and can be observed next to the image; bars, 100 μm. *(B)* High magnification confocal micrograph demonstrating MSV localization within the cardiomyocytes, particle fluorescence (green) was extracted from the micrograph and can be observed next to the image; bars, 40 μm. *(C)* Z-stack and tridimensional rendering analysis was performed to demonstrate the internalization and high density of MSV distribution within the tissue; bar, 40 μm. (D) High magnification z-stack micrographs of cardiomyocytes presenting MSVs internalization beneath the cellular membrane and intracellular microtubule trafficking to the perinuclear region of the cell; bars, 10 μm.

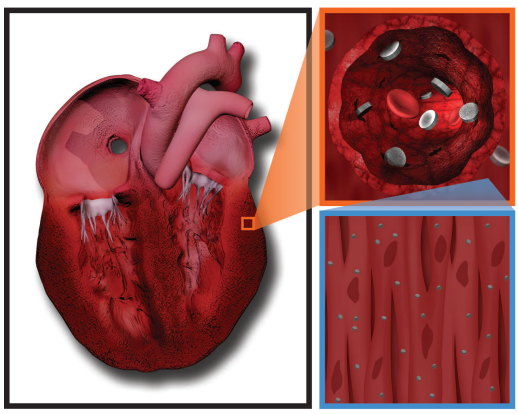

Figure 6 Schematic presentation of the mechanism of accumulation and intravascular transport dynamics of mesoporous silicon vector (MSV) to the failing heart. After intravenous injection, the rationally designed MSVs transport through the circulatory system and, as a result of their size, shape, and chemical modifications, avoid reticuloendothelial system uptake and undergo vascular margination and extravasation from dysfunctional fenestrated capillaries present in the failing heart, where they reach the cardiomyocytes.

pathway that couple to a phagosome and prompt its maturation and centripetal movement toward perinuclear regions.[31]

Another phenomenon observed in HCM, in HCMEC, and in lower rates in HCASMC, was the particle trafficking within adjacent cells. This phenomenon has been described as a mechanism of membrane extension between cells, in which different materials and signals are shared through channels known as tunnelling nanotubes.[32] Previous findings have described MSV internalization, perinuclear migration, and intercellular trafficking in human umbilical vein endothelial cells.[32,33] Nevertheless, observations of MSV accumulation in perinuclear regions of HCM, HCF, HCASMC, and RCM, have not been described before. In this study we also documented for the first time MSV trafficking to adjacent cells in HCM and HCASMC. The MSV uptake patterns are cell-type dependent; the unique features that determine dynamics are not known but likely result from the unique physical and biological features corresponding to each cell type.

Mesoporous silicon vectors are non-toxic for cardiac cells

To determine the safety of MSVs, the cytotoxicity of MSV in cultured human cell lines was examined. Flow cytometry analysis showed negligible increases in early apoptotic and necrotic

populations at dose increments, amounting less than 2.5% of cells undergoing apoptosis or necrosis.

Cytotoxic potential was examined by determining the impact of MSVs on progression of the cell cycle. At the highest dose of MSVs, no cell cycle arrest at G2-M was found. Defects at G2-M are a prerequisite step for apoptosis, allowing a damaged cell to enter mitosis and undergo apoptosis.[34] Studies previously published by our group have demonstrated the absence of toxicity and organelle ultrastructural damage in different cell types following internalization of MSVs, similarly, *in vivo* studies wherein repeated intravenous administration of MSVs over a 6-month period showed no evidence of organ or tissue injury.[35–37] Furthermore, echocardiograms did not reveal any alterations in ejection fraction after administration of MSVs, demonstrating the innocuousness of the nanoconstruct on cardiac contractility. As a result of its biodegradability into harmless silicic acid byproducts, MSV proves safe for cardiovascular applications.[35–37]

Heightened accumulation of mesoporous silicon vector in failing rather than normal myocardium

Similar to what is observed in the cancer vascular microenvironment, during the pathophysiological processes present in heart failure, vascular injury and endothelial dysfunction are produced.[38] Therefore, it was reasonable to assume that nanoconstructs would accumulate in failing myocardium. Compared with control hearts, accumulation of MSVs was significantly increased in failing myocardium (14-fold increase). The mechanism of accumulation in heart failure is not known, but it is consistent with disruption of the endothelial barrier, causing a cardiac enhanced permeability and retention (CEPR) effect associated with the pathological state. After extravasation, cardiomyocytes interact with nanoconstructs in the same manner as that observed *in vitro,* presenting intracellular uptake and resembling microtubule-based transport to the perinuclear region of cardiomyocytes.

Current experimental approaches for the treatment of heart failure involve supplying of proteins, growth factors, and drugs in an unstable and rapidly degradable plain form, decreasing the therapeutic effect and accumulation in the desired tissue.[2,39,40] It has been proven in previous studies that the encapsulation of therapeutic agents within nanoparticles may help overcome these limitations, modifying its pharmacokinetic properties, which in turn enable the reduction of clearance, prolonged circulation half-life and controlled sustained release compared with conventional formulations.[40] Genetic approaches such as the delivery of SERCA2a encased in an adenoviral vector, have failed to show improved patient outcomes in clinical trials, and have been associated with immunogenicity and low concentration of the gene product in the myocardium.[2] Nanotechnology platforms provide an alternative for stable and protected intracellular delivery of genetic material without degradation and immunogenicity, which in combination with specific genetic sequences and promoters has the potential to enable a site-specific effect in failing myocardium.

Future studies are currently focused on developing a variety of nanoparticles and characterizing accumulation and biodistribution. It is likely that specific nanoconstructs could be created to target myocytes, fibroblasts, or endothelial cells in a more specific fashion in addition to creating particles that are specifically designed for protein or gene delivery. In the present study, we used a model of non-ischaemic cardiomyopathy that is traditionally used to induce hypertension and cardiac fibrotic response secondary to the increase of angiotensin II, which in turn is known to cause cardiac hypertrophy and dysfunction during essential hypertension.[14,41] Nanoparticle accumulation dynamics may be the result of this specific model. Different heart failure states exist and future applications of nanotechnology-based delivery systems will have to be explored in other cardiomyopathy models, as the accumulation dynamics of nanoconstructs in non-ischaemic and ischaemic states may differ owing to important pathophysiological differences.

In summary, cardiac cells are able to internalize and traffic MSVs to the perinuclear cellular regions, and this process was found to be non-toxic. Furthermore, MSVs successfully accumulated in increased amounts in failing hearts compared with normal hearts. These findings have several implications in heart failure. First, accumulation of nanoconstructs in damaged heart will allow the use of insoluble hydrophobic drugs. Second, these findings open the possibility of intracellular delivery of proteins or genetic material into failing myocardium to create new therapies. Third, imaging and diagnostic systems, such as contrast agents and nanosensors, could allow for the examination of disease at the cellular level. Finally, the use of novel nanoconstructs such as MSVs, offer the potential of engineering combinatorial theranostic approaches, wherein co-encapsulation of drugs, proteins, genetic material, and imaging moieties result in novel preventive, therapeutic, and diagnostic strategies. Together, these observations form the basis for future nanotherapeutic or diagnostic approaches in heart failure.

Acknowledgements

G.U.R.E. and V.S-I. are grateful for support from Tecnológico de Monterrey. V.S-I. also appreciates the support from the Consejo Nacional de Ciencia y Tecnología (CONACyT, 490202/278979). M.F. is grateful for the support of the Ernest Cockrell Jr Presidential Distinguished Chair. Matthew G. Landry is acknowledged for manuscript schematic. The authors acknowledged the Nanofabrication Core of the Houston Methodist Research Institute for porous silicon microparticle fabrication and surface chemical modification.

Supplementary Information

Additional Supporting Information may be found in the online version of this article:

Figure S1. Tridimensional rendering of human cardiovascular cells showing cellular co-localization and density of nanoconstructs.

Figure S2. To determine MSV cytotoxicity, human cardiovascular cells were treated with several dosages of MSV (1:1, 1:25, 1:150, 1:250) for 24 h.

Figure S3. Cell cycle analysis in MSV-treated human cardiovascular cells. To determine cell cycle alterations cells were incubated with different dosages of MSVs (1:1, 1:25, 1:150, 1:250) for 24h.

Figure S4. Representative bar graphs of (A) cytotoxicity in MSV-treated human cardiovascular cells and (B) cell cycle analysis in MSV-treated human cardiovascular cells.
Figure S5. Mouse with control normal heart and mouse with failing heart.
Figure S6. Biodistribution of the MSVs measured by epifluorescence.
Video S1. HCM incubated with MSVs during a 12-h time-lapse microscopy assay.
Video S2. HCF incubated with MSVs during a 12 h time-lapse microscopy assay, showing intracellular particle trafficking and perinuclear sequestration.
Video S3. HCASMC incubated with MSVs during a 12 h time-lapse microscopy assay, showing particle trafficking between adjacent cells.
Video S4. HCMEC incubated with MSVs during a 12-h time-lapse microscopy assay, showing intracellular trafficking of particles to the perinuclear region of the cell.
Method S1. Supplementary methods.

Funding

This work was supported by funding from the George and Angelina Kostas Research Center for Cardiovascular Nanomedicine, Department of Defense grants W81XWH-09-1-0212 and W81XWH-12-1-0414, as well as National Institute of Health grants NIH U54CA143837 and U54CA151668.
Conflict of interest: none declared.

References

1. Miller LW. Limitations of current medical therapies for the treatment of heart failure. *Rev Cardiovasc Med* 2003;**4**(Suppl 2):S21–S29.
2. Giacca M, Baker AH. Heartening results: the CUPID gene therapy trial for heart failure. *Mol Ther* 2011;**19**:1181–1182.
3. Matsumura Y, Maeda H. A new concept for macromolecular therapeutics in cancer chemotherapy: mechanism of tumoritropic accumulation of proteins and the antitumor agent smancs. *Cancer Res* 1986;**46**:6387–6392.
4. Dvir T, Bauer M, Schroeder A, Tsui JH, Anderson DG, Langer R, Liao R, Kohane DS. Nanoparticles targeting the infarcted heart. *Nano Lett* 2011;**11**:4411–4414.
5. Ruiz-Esparza GU, Flores-Arredondo JH, Segura-Ibarra V, Torre-Amione G, Ferrari M, Blanco E, Serda RE. The physiology of cardiovascular disease and innovative liposomal platforms for therapy. *IntJ Nanomed* 2013;**8**:629–640.
6. Taimeh Z, Loughran J, Birks EJ, Bolli R. Vascular endothelial growth factor in heart failure. *Nat Rev Cardiol* 2013;**10**:519–530.
7. Liesmaa I, Kuoppala A, Shiota N, Kokkonen JO, Kostner K, Mayranpaa M, Kovanen PT, Lindstedt KA. Increased expression of bradykinin type-1 receptors in endothelium of intramyocardial coronary vessels in human failing hearts. *Am J Physiol Heart Circ Physiol* 2005;**288**:H2317–H2322.
8. Giordano FJ. Oxygen, oxidative stress, hypoxia, and heart failure. *J Clin Invest* 2005;**115**:500–508.
9. Torre-Amione G. Immune activation in chronic heart failure. *Am J Cardiol* 2005;**95**:3C–8C.
10. Tasciotti E, Liu X, Bhavane R, Plant K, Leonard AD, Price BK, Cheng MM, Decuzzi P, Tour JM, Robertson F, Ferrari M. Mesoporous silicon particles as a multistage delivery system for imaging and therapeutic applications. *Nat Nanotechnol* 2008;**3**:151–157.
11. Blanco E, Sangai T, Hsiao A, Ferrati S, Bai L, Liu X, Meric-Bernstam F, Ferrari M. Multistage delivery of chemotherapeutic nanoparticles for breast cancer treatment. *Cancer Lett* 2013;**334**:245–252.
12. Silva-Platas C, Garcia N, Fernandez-Sada E, Davila D, Hernandez-Brenes C, Rodriguez D, Garcia-Rivas G. Cardiotoxicity of acetogenins from *Persea americana* occurs through the mitochondrial permeability transition pore and caspase-dependent apoptosis pathways. *J Bioenerg Biomembr* 2012;**44**:461–471.
13. Oestreicher EM, Martinez-Vasquez D, Stone JR, Jonasson L, Roubsanthisuk W, Mukasa K, Adler GK. Aldosterone and not plasminogen activator inhibitor-1 is a critical mediator of early angiotensin II/NG-nitro-L-arginine methyl ester-induced myocardial injury. *Circulation* 2003;**108**:2517–2523.
14. Garcia-Rivas G, Youker KA, Orrego C, Flores-Arredondo J, Guerrero-Beltran CE, Cordero-Reyes A, Gutierrez-Uribe JA, Garcia M, Serna-Saldivar SO, Torre-Amione G. Standardized extracts from black bean coats (*phaseolus vulgaris* l.) prevent adverse cardiac remodeling in a murine model of non-ischemic cardiomyopathy. *RSC Advances* 2015;**5**:90858–90865.
15. Godin B, Chiappini C, Srinivasan S, Alexander JF, Yokoi K, Ferrari M, Decuzzi P, Liu X. Discoidal porous silicon particles: Fabrication and biodistribution in breast cancer bearing mice. *Adv Funct Mater* 2012;**22**:4225–4235.
16. van de Ven AL, Kim P, Haley O, Fakhoury JR, Adriani G, Schmulen J, Moloney P, Hussain F, Ferrari M, Liu X, Yun SH, Decuzzi P. Rapid tumoritropic accumulation of systemically injected plateloid particles and their biodistribution. *J Control Release* 2012;**158**:148–155.
17. Decuzzi P, Godin B, Tanaka T, Lee SY, Chiappini C, Liu X, Ferrari M. Size and shape effects in the biodistribution of intravascularly injected particles. *J Control Release* 2010;**141**:320–327.
18. Decuzzi P, Ferrari M. The receptor-mediated endocytosis of nonspherical particles. *Biophys J* 2008;**94**:3790–3797.
19. Shen J, Xu R, Mai J, Kim HC, Guo X, Qin G, Yang Y, Wolfram J, Mu C, Xia X, Gu J, Liu X, Mao ZW, Ferrari M, Shen H. High capacity nanoporous silicon carrier for systemic delivery of gene silencing therapeutics. *ACS Nano* 2013;**7**:9867–9880.
20. Serda RE, Gu J, Burks JK, Ferrari K, Ferrari C, Ferrari M. Quantitative mechanics of endothelial phagocytosis of silicon microparticles. *Cytometry A* 2009;**75A**:752–760.
21. Serda RE, Ferrati S, Godin B, Tasciotti E, Liu XW, Ferrari M. Mitotic trafficking of silicon microparticles. *Nanoscale* 2009;**1**:250–259.
22. Ferrati S, Serda RE, Bean A, Ferrari M. Intracellular trafficking of nano-carriers. In *Nemb2010: Proceedings of the Asme First Global Congress on Nanoengineering for Medicine and Biology - 2010*. The American Society of Mechanical Engineers Digital Collection. Houston Texas, USA. 2010:105–107.
23. Ferrati S, Mack A, Chiappini C, Liu XW, Bean AJ, Ferrari M, Serda RE. Intracellular trafficking of silicon particles and logic-embedded vectors. *Nanoscale* 2010;**2**:1512–1520.
24. Serda RE, Gu J, Bhavane RC, Liu X, Chiappini C, Decuzzi P, Ferrari M. The association of silicon microparticles with endothelial cells in drug delivery to the vasculature. *Biomaterials* 2009;**30**:2440–2448.
25. James TN, Terasaki F, Pavlovich ER, Vikhert AM. Apoptosis and pleomorphic micromitochondriosis in the sinus nodes surgically excised from five patients with the long qt syndrome. *Jo Lab Clin Med* 1993;**122**:309–323.
26. Blaes N, Crouzet B, Bourdillon MC, Boissel JP. Comparative phagocytosis in culture of aortic smooth muscle cells and fibroblasts from rat. *Proc Soc Exp Biol Med* 1982;**170**:453–458.
27. Gao C, Xie R, Li W, Zhou J, Liu S, Cao F, Liu Y, Ma R, Si Y, Liu Y, Bi Y, Gilbert GE, Shi J. Endothelial cell phagocytosis of senescent neutrophils decreases procoagulant activity. *Thromb Haemos* 2013;**109**:1079–1090.
28. Babaev VR, Popkova VM, Antonov AS, Repin VS. [Quantitative evaluation of the phagocytic activity of endothelial cells in culture]. *Biull Eksp Biol Med* 1986;**101**:728–730 (in Russian).
29. Privalova LI, Katsnelson BA, Osipenko AB, Yushkov BN, Babushkina LG. Response of a phagocyte cell system to products of macrophage breakdown as a probable mechanism of alveolar phagocytosis adaptation to deposition of particles of different cyto-toxicity. *Environ Health Persp* 1980;**35**: 205–218.
30. Proffitt RT, Williams LE, Presant CA, Tin GW, Uliana JA, Gamble RC, Baldeschwieler JD. Liposomal blockade of the reticuloendothelial system: improved tumor imaging with small unilamellar vesicles. *Science* 1983;**220**:502–505.
31. Harrison RE, Bucci C, Vieira OV, Schroer TA, Grinstein S. Phagosomes fuse with late endosomes and/or lysosomes by extension of membrane protrusions along microtubules: Role of rab7 and rilp. *Mol Cell Biol* 2003;**23**:6494–6506.
32. Ferrati S, Shamsudeen S, Summers HD, Rees P, Abbey JV, Schmulen J, Liu X, Wong ST, Bean AJ, Ferrari M, Serda RE. Inter-endothelial transport of microvectors using cellular shuttles and tunneling nanotubes. *Small* 2012;**8**: 3151–3160.
33. Serda RE, Gu J, Burks JK, Ferrari K, Ferrari C, Ferrari M. Quantitative mechanics of endothelial phagocytosis of silicon microparticles. *Cytometry A* 2009;**75**:752–760
34. Cuddihy AR, O'Connell MJ. Cell-cycle responses to DNA damage in g2. *Int Rev Cytol.* 2003;**222**:99–140.
35. Martinez JO, Parodi A, Liu X, Kolonin MG, Ferrari M, Tasciotti E. Evaluation of cell function upon nanovector internalization. *Small* 2013;**9**: 1696–1702.

36. Martinez JO, Boada C, Yazdi IK, Evangelopoulos M, Brown BS, Liu X, Ferrari M, Tasciotti E. Short and long term, *in vitro* and *in vivo* correlations of cellular and tissue responses to mesoporous silicon nanovectors. *Small* 2013;**9**:1722–1733.
37. Shen J, Xu R, Mai J, Kim H-C, Guo X, Qin G, Yang Y, Wolfram J, Mu C, Xia X, Gu J, Liu X, Mao Z-W, Ferrari M, Shen H. High capacity nanoporous silicon carrier for systemic delivery of gene silencing therapeutics. *ACS Nano* 2013;**7**:9867–9880.
38. Fischer D, Rossa S, Landmesser U, Spiekermann S, Engberding N, Hornig B, Drexler H. Endothelial dysfunction in patients with chronic heart failure is independently associated with increased incidence of hospitalization, cardiac transplantation, or death. *Eur Heart J* 2005;**26**:65–69.
39. Hastings CL, Roche ET, Ruiz-Hernandez E, Schenke-Layland K, Walsh CJ, Duffy GP. Drug and cell delivery for cardiac regeneration. *Adv Drug Deliv Rev* 2015;**84**:85–106.
40. Kadam RS, Bourne DW, Kompella UB. Nano-advantage in enhanced drug delivery with biodegradable nanoparticles: Contribution of reduced clearance. *Drug Metab Dispos* 2012;**40**:1380–1388.
41. Crowley SD, Gurley SB, Herrera MJ, Ruiz P, Griffiths R, Kumar AP, Kim HS, Smithies O, Le TH, Coffman TM. Angiotensin ii causes hypertension and cardiac hypertrophy through its receptors in the kidney. *Proc Natl Acad Sci U S A* 2006;**103**:17985–17990.